International Journal of Minerals, Metallurgy and Materials
Volume 27, Number 1, January 2020, Page 91
https://doi.org/10.1007/s12613-019-1908-4

Hydroxylated graphene quantum dots as fluorescent probes for sensitive detection of metal ions

Qiang Ge[1)], *Wen-hui Kong*[1)], *Xin-qian Liu*[1)], *Ying-min Wang*[1)], *Li-feng Wang*[1)], *Ning Ma*[2)], *and Yan Li*[1)]

1) Department of Inorganic Nonmetallic Material, School of Materials Science and Engineering, University of Science and Technology Beijing, Beijing 100083, China
2) College of Materials Science and Chemical Engineering, Harbin Engineering University, Harbin 150001, China
(Received: 29 May 2019; revised: 1 August 2019; accepted: 16 August 2019)

Abstract: Highly sensitive methods are important for monitoring the concentration of metal ions in industrial wastewater. Here, we developed a new probe for the determination of metal ions by fluorescence quenching. The probe consists of hydroxylated graphene quantum dots (H-GQDs), prepared from GQDs by electrochemical method followed by surface hydroxylation. It is a non-reactive indicator with high sensitivity and detection limits of 0.01 μM for Cu^{2+}, 0.005 μM for Al^{3+}, 0.04 μM for Fe^{3+}, and 0.02 μM for Cr^{3+}. In addition, the low biotoxicity and excellent solubility of H-GQDs make them promising for application in wastewater metal ion detection.

Keywords: graphene quantum dots; surface hydroxylation; metal ions detection; fluorescent probes

1. Introduction

In recent years, optical detection techniques, especially fluorescence spectroscopic methods, have been attracting much attention and have been widely investigated for their applications in the detection of various analytes, such as neutral molecules, heavy metal ions, enzymes, and anions [1]. In particular, fluorescence sensing is the method of choice because of its rapid signal acquisition, high sensitivity, and easy operation, and it can identify specific molecules via the interaction between the sensing material and the target [2]. Fluorescent probes are generally divided into two categories: reactive and non-reactive indicators. Reactive indicators are based on molecular reactivity instead of molecular recognition and achieve a high chemical selectivity in complicated biological and environmental systems [3]. Thus, high sensitivity is the main advantage of these indicators; however, the alteration of the utilized materials is irreversible. On the other hand, non-reactive indicators are based on non-covalent physical interactions, such as electrostatic, π–π, donor–acceptor, hydrogen bonding, hydrophobic, hydrophilic, and coordination interactions, which leave the structure of the sensing material unchanged; however, their sensitivity is usually lower than that of reactive indicators [4]. Hence, the development of novel highly sensitive non-reactive indicators is of great interest.

Recently, graphene quantum dots (GQDs) have shown potential applications in many fields, such as optoelectronic devices, bioimaging, and biomedical research, on account of their outstanding fluorescent properties, excellent chemical and physical stability, and low toxicity [5–7]. In particular, surface-active oxygen functional groups such as epoxy groups, hydroxyl, and carboxyl have found application in sensing devices, especially for metal ion detection [8–9]. Because the surface hydroxyl and carboxyl groups increase the electronegativity of GQDs, metal cations can interact with these groups via electrostatic forces. The following electron transfer processes result in the agglomeration of GQDs or change in surface states and consequently fluorescence enhancement or quenching, allowing GQDs to detect various ions, such as Al^{3+} [10], Fe^{3+} [11], Hg^{2+} [12], Cr^{6+} [13], Cu^{2+} [14], and Pb^{2+} [15], with high sensitivity [16]. However, there is still room for improvement in terms of sensitivity compared with reactive indicators. To achieve a highly effi-

Corresponding author: Yan Li E-mail: liyan2011@ustb.edu.cn

cient and sensitive fluorescent biosensor, two basic requirements must be met: (1) strong fluorescence and (2) the existence of a sufficient number of metal-binding sites. For most GQDs, fluorescence results from quantum size and surface state effects [17]. According to the previous understanding of the luminescence nature of quantum dots, when their total surface oxygen level increases, the fluorescence intensity usually decreases [18]. Thus, simultaneously increasing the fluorescence intensity and the number of meta-binding sites is not possible. Utilizing graphene quantum dots–aptamer probe and graphene oxide platform as a fluorescent nanosensor for the detection of lead(II) ion, Qian *et al.* [19] found a wide linear span of up to 400 nM and an ultra-low detection limit of 0.6 nM. However, in a recent study, we showed that different hybridized surface states lead to different fluorescence colors. In particular, a high content of hybrid state from C−OH bonds as well as graphene core not only results in a GQD fluorescence blue shift but also increases the fluorescence intensity [20]. This important result lays a foundation for further research in the design of highly sensitive GQD-based biosensors.

In this work, we first prepared GQDs by electrochemical method and then treated them by surface hydroxylation to obtain H-GQDs, which had a higher number of hydroxyl groups but the same original structure as the GQDs. The H-GQDs proved to be highly sensitive in the detection of Cu^{2+}, Al^{3+}, Fe^{3+}, and Cr^{3+} ions by fluorescence quenching. We studied the fluorescence quenching mechanism and compared our results to those previously reported for other carbon nanomaterials.

2. Experimental

2.1. Preparation of GQDs and H-GQDs

Graphene quantum dots were prepared by cyclic voltammetry on a CHI660D electrochemical workstation [21]. The working electrode was a graphite rod, and the counter electrode was a platinum electrode. We used 20 mL PBS buffer solution (pH = 7, 0.1 M) as the electrolyte. The CV potential was within ±5.0 V, the scan rate was set as 0.5 V/s, and the scan time was 3 d. After scanning, the solution was filtered by a membrane (220 nm), and then dialyzed with a cellulose ester membrane bag (3500 Da) for 4 d. The deionized water was changed every 2 h, and the GQD aqueous solutions were obtained.

The H-GQDs were prepared as follows: A part of GQDs (5 mL) was added to 30 μL H_2O_2 (30wt%). The mixture was stirred with an irradiated ultraviolet lamp (the wavelength was 254 nm, 18 W) for 24 h. Afterward, the solution was immediately dialyzed for 4 d to remove excess H_2O_2.

2.2. Detection of Cu^{2+}, Al^{3+}, Fe^{3+}, and Cr^{3+}

Stock standard solutions of Cu^{2+}, Al^{3+}, Fe^{3+}, and Cr^{3+} (0.01 M) were prepared by dissolving a certain amount of $CuCl_2$, $AlCl_3$, $FeCl_3$, and $CrCl_3{\cdot}6H_2O$, respectively, in deionized water. The ion solution was diluted and added to H-GQDs (2 mL) according to different concentration gradients. After sufficient mixing, the solutions were transferred to fluorescence cuvettes, and the respective fluorescence spectra were recorded.

The limit of detection (LOD) was calculated as follows: the prepared 0.01 M Cu^{2+}, Al^{3+}, Fe^{3+}, and Cr^{3+} solutions were added into H-GQDs solutions (2 mL).

$$\mathrm{LOD} = C_1 = \frac{C_0 V_0}{V_1} \tag{1}$$

where C_0 is the concentration of the metal ions (C_0 = 0.01 M), and V_0 is the volume of the metal ions, C_1 is the detected concentration, and V_1 is the volume of H-GQDs (V_1 = 2 mL). The error was produced by the pipette, and the instructions of the pipette reported an allowable error of 5 μL, which was ±8.0%.

2.3. Characterization methods

Transmission electron microscopy (TEM, H-7650B) analyses were carried out using an electron microscope at 120 kV. The sample for measurement was prepared by depositing GQDs and H-GQDs aqueous solution on silicon wafers on a drying oven at 40°C for 2 d. Fourier-transform infrared (FT-IR) spectra were recorded by a NEXUS spectrometer 670 using KBr pellets. The Raman spectra were obtained using an RM2000 microscopic confocal Raman spectrometer under He−Ne laser with the excitation wavelength at 632.8 nm. The photoluminescence (PL) spectra of the samples were obtained using an F97 Pro spectrophotometer. X-ray photoelectron spectroscopy (XPS) analysis was carried out using an ESCALAB 250Xi photoelectron spectrometer with Al monochromated K_α radiation.

3. Results and discussion

The morphologies of GQDs and H-GQDs were characterized by TEM, and the images are shown in Fig. 1. After surface hydroxylation, H-GQDs maintained the original size morphology, except some smaller-sized H-GQDs produced after hydroxylation. The average diameters of GQDs and H-GQDs are 2.81 nm and 2.89 nm, respectively. As can be seen from Fig. 2(a), the FT-IR spectra of GQDs and H-GQDs showed many stretching vibration bands correspond-

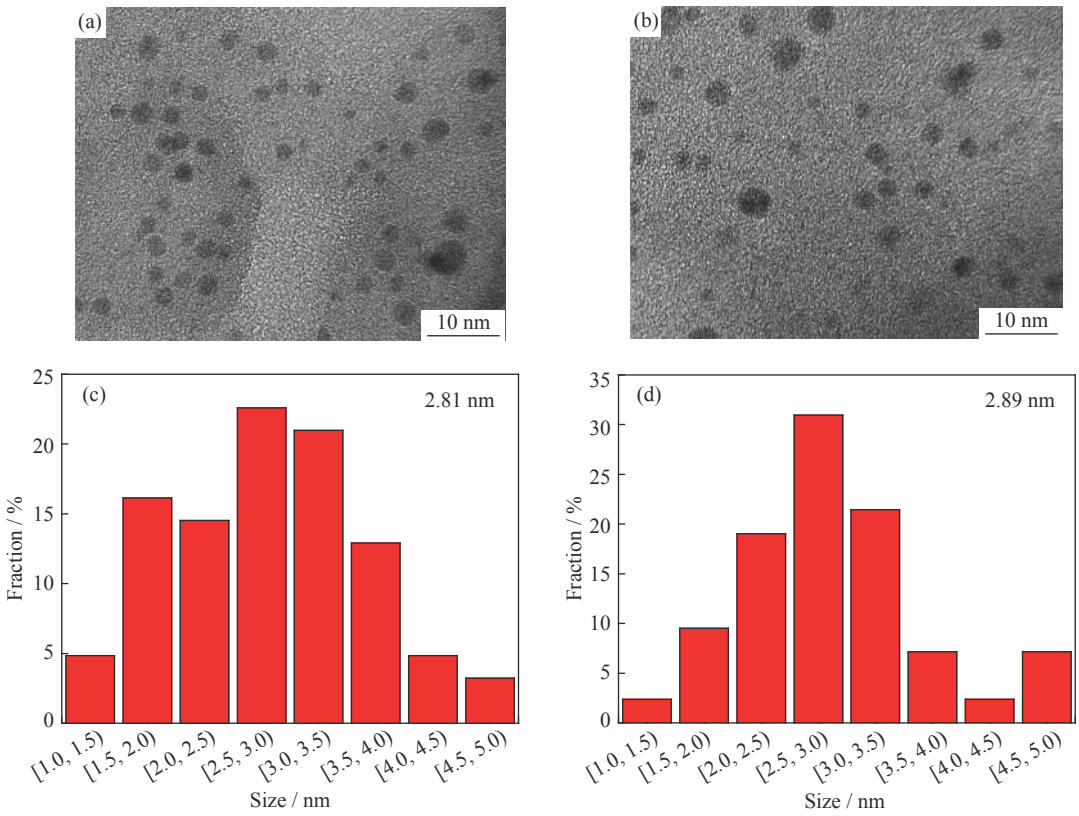

Fig. 1. TEM images and histograms of size distribution of (a, c) GQDs and (b, d) H-GQDs.

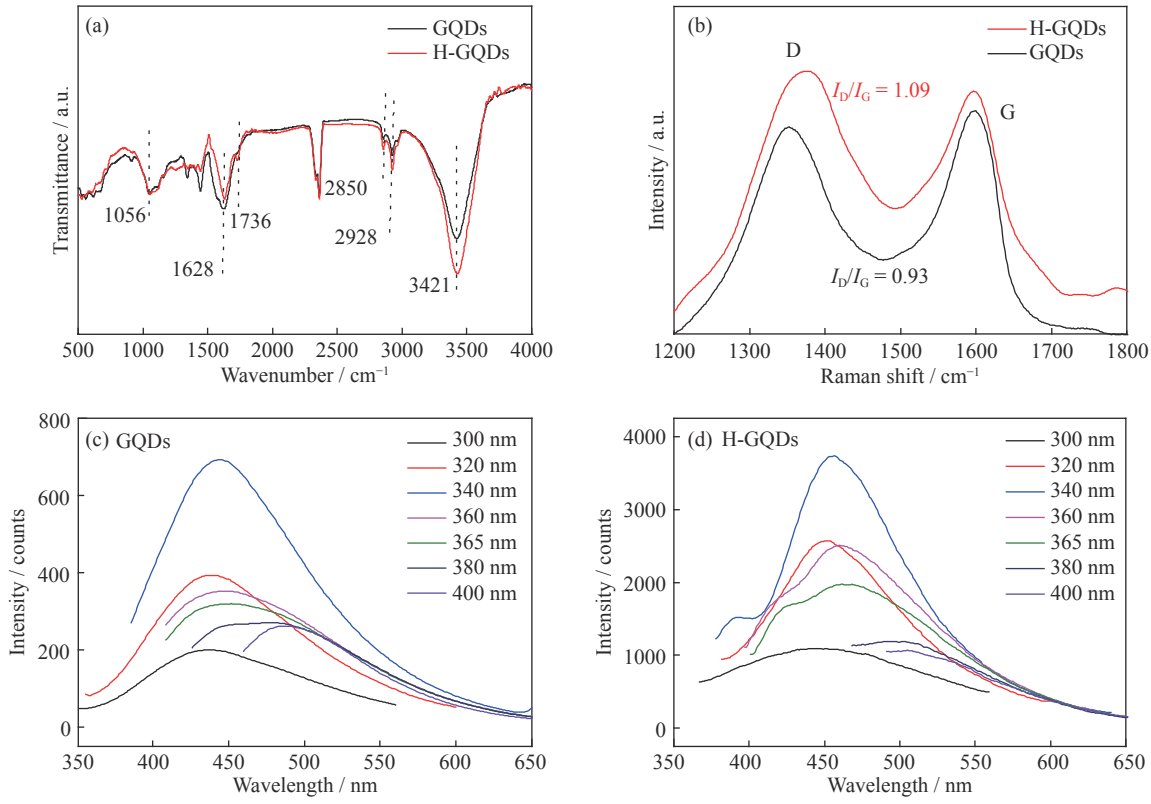

Fig. 2. (a) FT-IR and (b) Raman spectra of GQDs and H-GQDs, and PL spectra of (c) GQDs and (d) H-GQDs with the excited wavelength at 300–400 nm.

ing to oxygen-containing surface groups [21], namely, epoxy (C−O−C, 1056 cm^{-1}), carbonyl (C=O, 1736 cm^{-1}), and hydroxyl groups (C−OH, 3421 cm^{-1}) [22−23]. Notably, the C−OH vibration peak of H-GQDs was more intense than that of GQDs, indicating that the hydroxyl groups were successfully introduced. Moreover, C−C was not observed because the vibration of the same nuclear diatomic pair was very weak in the FT-IR spectrum. The Raman spectra of GQDs and H-GQDs were shown in Fig. 2(b), both the two samples showed two main peaks at approximately 1350 cm^{-1} (D-band) and 1597 cm^{-1} (G-band). The D-band is related to the structural defects and partially disordered structures of the sp^2 domains, and the G-band depends on the E_{2g} vibration mode of the sp^2 carbon domains. The strength of the G-band is defined as I_G, and the strength of the D-band is defined as I_D. The ratio of I_D/I_G in Raman spectra is used to evaluate the disorder in graphene materials [24]. In Fig. 2(b), a clear red shift of the D band and a higher I_D/I_G value (1.09) was observed in the Raman spectrum of H-GQDs, while the I_D/I_G value for GQDs was lower (0.93), further suggesting that the newly introduced hydroxyl groups increased the surface defects. The change in the surface C−OH contents of H-GQDs was calculated by XPS, as shown in Fig. 3. Based on the FT-IR results, the C 1s peak of GQDs and H-GQDs could be deconvoluted into four components: C=C/C−C (284.4 eV), C−OH (285.6 eV), C−O−C (287.4 eV), and C=O (288.2 eV) [25]. Interestingly, after the hydroxylation, the number of C−O−C groups slightly decreased (from 11.91% for GQDs to 8.05% for H-GQDs), whereas that of C=O groups remained almost unchanged, and the C−OH content significantly increased (from 19.27% for GQDs to 29.05% for H-GQDs). These results indicate that our approach allows to modify the surface groups of GQDs without destroying the internal structure.

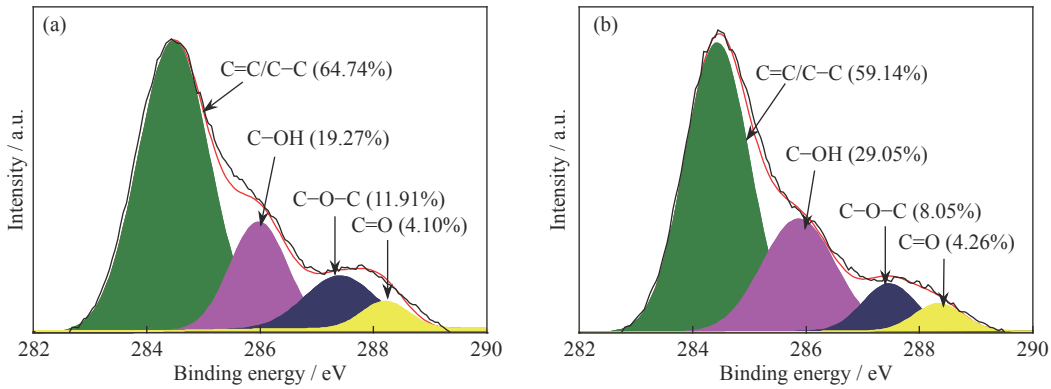

Fig. 3. C 1s XPS spectra of GQDs (a) and H-GQDs (b).

The GQDs and H-GQDs (19.27% and 29.05%, a high content of hydroxyl groups, as revealed by XPS) both exhibited the strongest PL at about 450 nm when the excitation wavelength was 340 nm, as shown in Figs. 2(c) and 2(d). This indicates that H-GQDs and GQDs have a similar band gap. Based on linear extrapolation of the absorption spectra of solutions of H-GQDs, the band gaps were calculated by plotting the square or square root of the absorption energy ($\alpha h\upsilon$, where α is the absorbance and $h\upsilon$ is the photon energy) against $h\upsilon$, which enabled the determination of the direct or indirect band gap energy (Fig. 4), the band gap was calculated to be 2.91 eV [21]. The PL of H-GQDs can be ascribed to an electronic transition between the valence and conduction bands. A small peak at about 380 nm was also observed (Fig. 2(d)), which can be ascribed to some smaller-sized H-GQDs produced, in agreement with the TEM result [26]. The PL spectra are consistent with the result of our previous study, demonstrating that hydroxyl groups related hybridized states were responsible for the blue emission at 440 nm when the wavelength was about 360 nm. Furthermore, the PL intensity of H-GQDs at 450 nm was about 5.5 times higher than that of the GQDs, which provides a wider ion detection range. During the hydroxylation process, a large number of hydroxyl groups in GQDs are induced by hydroxide radical from H_2O_2. After oxidation, some of the interrupted π-conjugated electron structures will recombine and cause an increase in π-electron delocalization, which is more easily excited and then leads to a high PL intensity of H-GQDs [20].

Because the highest emission was 450 nm when the excitation wavelength was 340 nm, 340 nm was selected as the excitation wavelength to increase the detection of H-GQDs. The quantitative detection of Cu^{2+}, Al^{3+}, Fe^{3+}, and Cr^{3+} ions was performed under the optimized conditions. As can be seen from the PL spectra of H-GQDs in the presence of Cu^{2+}, Al^{3+}, Fe^{3+}, and Cr^{3+} ions (Figs. 5(a)–5(d), respectively), the PL of H-GQDs was dependent on the metal ion concentration. With an increase in the concentrations of Cu^{2+}, Al^{3+},

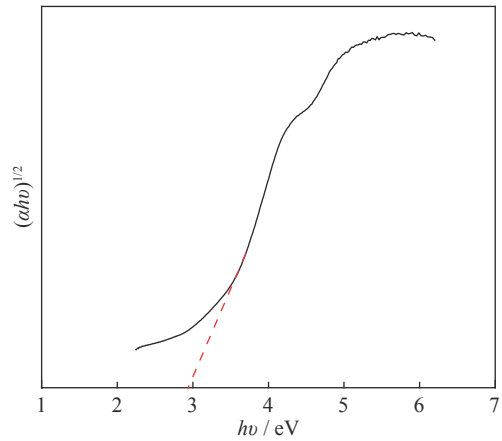

Fig. 4. Plots of $(\alpha h\upsilon)^{1/2}$ against photon energy ($h\upsilon$) for the H-GQDs solution, where α is the absorbance.

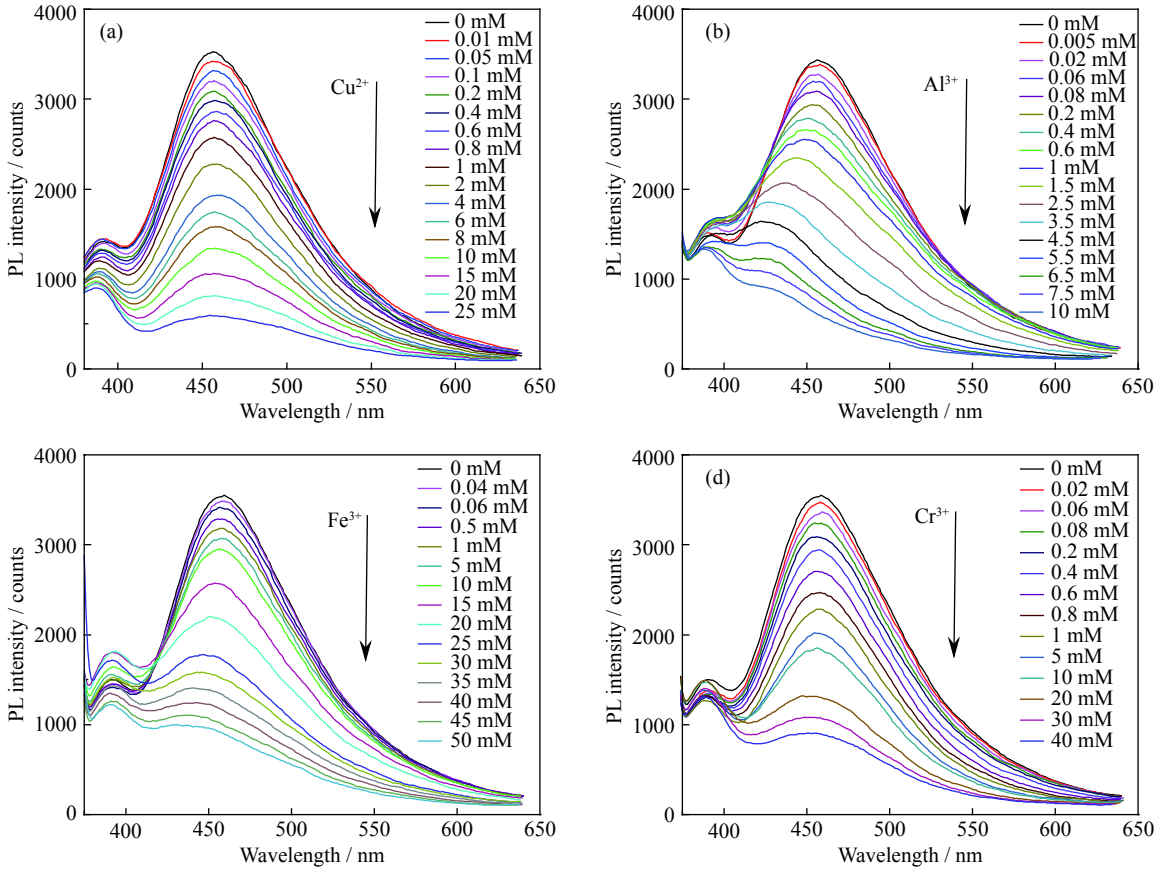

Fig. 5. PL spectra of H-GQDs in the presence of (a) Cu^{2+}, (b) Al^{3+}, (c) Fe^{3+}, and (d) Cr^{3+} at different concentrations (the excited wavelength for all samples was 340 nm).

Fe^{3+}, and Cr^{3+} ions, the PL intensity of H-GQDs gradually decreased but in different proportions. When the metal ion concentration reached 10 μM, the PL of H-GQDs containing Al^{3+} was almost quenched, whereas the PL intensity of H-GQDs containing Cu^{2+} and Cr^{3+} decreased by 62% and 63%, respectively, and that of H-GQDs containing Fe^{3+} decreased only by 17%. Moreover, different detection limits were observed for the four metal ions, namely, 0.01 μM for Cu^{2+}, 0.005 μM for Al^{3+}, 0.04 μM for Fe^{3+}, and 0.02 μM for Cr^{3+}. These values are much lower than those reported for most carbon materials, as summarized in Table 1, and comparable to those of reactive indicators. Stern-Volmer equation can be used to analyze the quenching effect quantitatively [27]:

$$F_0/F = 1 + K_{sv}[C] \quad (2)$$

Table 1. Detection limits of different sensing systems for Cu^{2+}, Al^{3+}, Fe^{3+}, and Cr^{3+}

Metal ion	Sensing probe	Detection limit	Ref.
Cu^{2+}	GQDs	0.226 μM	[15]
	N,S-GQDs	0.25 μM	[32]
	GQDs	0.33 μM	[33]
	Rhodamine B*	0.01 μM	[34]
	H-GQDs	0.01 μM	This work
Al^{3+}	CDs	0.05 μM	[10]
	Rhodamine chromone-based*	0.177 μM	[35]
	H-GQDs	0.005 μM	This work
Fe^{3+}	GO nanosheet	7.9 μM	[36]
	N-GQDs	0.09 μM	[37]
	Phosphonic acid-fluorine*	0.02 μM	[38]
	H-GQDs	0.04 μM	This work
Cr^{3+}	CDs-OH	0.06 μM	[39]
	GQDs	50 ppb	[40]
	Tripolyphosphate modified gold nanoparticles*	0.1 μM	[41]
	H-GQDs	0.02 μM	This work

Note: * Reaction-based probes.

where F_0 and F are the steady-state fluorescence intensities of H-GQDs in the absence and presence of the metal ions with the 450 nm excitation wavelength, K_{sv} is the Stern-Volmer quenching constant, and [C] is the concentration of quencher of metal ions. As observed in Fig. 6, the Stern-Volmer plots of fluorescence quenching of H-GQDs by met-

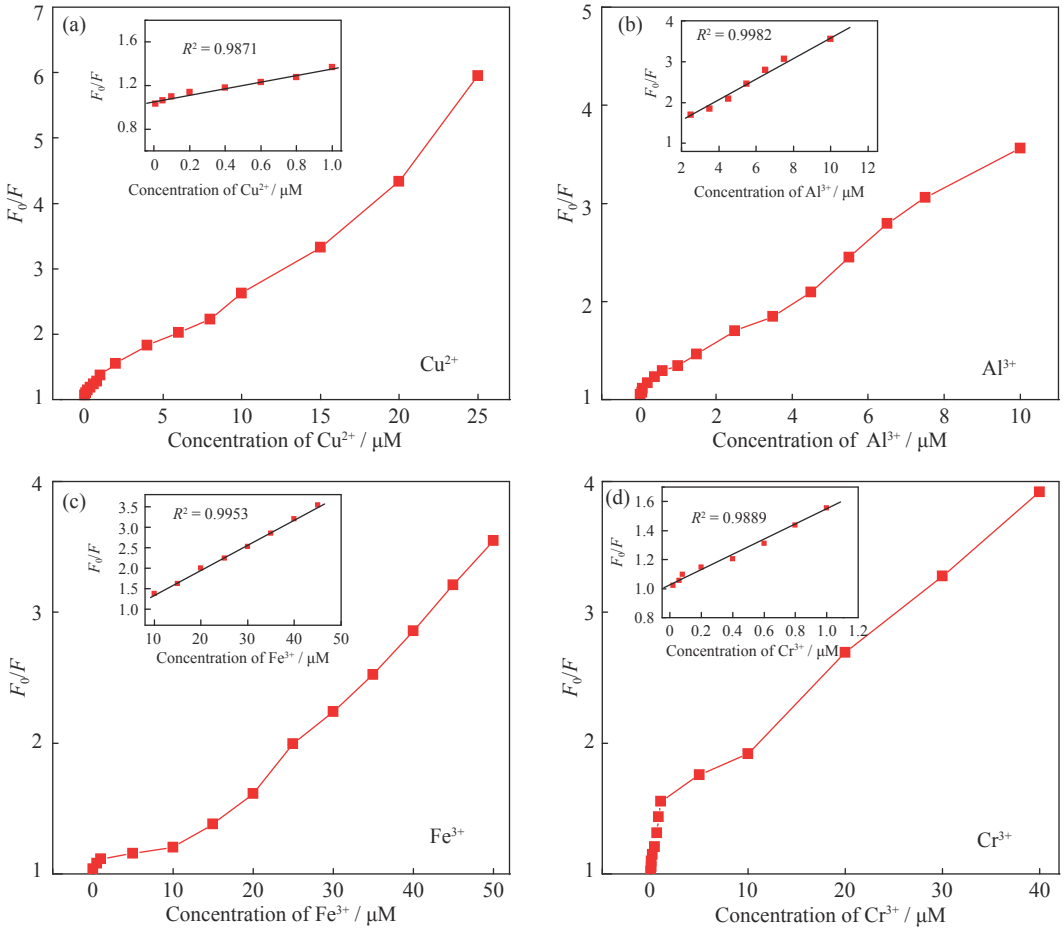

Fig. 6. Stern-Volmer plots of the fluorescence quenching of H-GQDs in aqueous solution by (a) Cu^{2+}, (b) Al^{3+}, (c) Fe^{3+}, and (d) Cr^{3+}.

al ions are not linear over the entire concentration range, but a good linearity is shown in the range of 0–1 μM for Cu^{2+}, 2–10 μM for Al^{3+}, 10–50 μM for Fe^{3+}, and 0–1.2 μM for Cr^{3+}, with R^2 = 0.9871, 0.9982, 0.9953, and 0.9889, respectively, as shown in the insets. Thus, static and dynamic quenching would be considered for the H-GQDs mechanism [28]. The static quenching results from the formation of non-fluorescent complex among H-GQDs and metal ions, and the dynamic quenching mechanism is governed by the collisions between the H-GQDs and metals ions [29].

According to the World Health Organization (WHO) report, 80% of diseases and 50% of child deaths worldwide are caused by drinking contaminated water. Excessive accumulation of heavy metals poses a serious threat to the environment and human health, especially in developing and emerging countries [30]. Moreover, according to the electroplating wastewater discharge standards, the concentrations of Cu^{2+}, Al^{3+}, Fe^{3+}, and Cr^{3+} cannot exceed 1, 5, 5, and 1.5 mg/L, respectively [31]. Notably, the detection limits of H-GQDs were far below these regulatory levels, suggesting their potential application for the determination of Cu^{2+}, Al^{3+}, Fe^{3+}, and Cr^{3+} ions in industrial wastewater.

Generally, the fluorescence quenching of non-reactive indicators induced by metal ions is due to a non-radiative electron/hole recombination through an effective electron transfer process [13] or due to aggregation [42]. According to Liu *et al.* [39], metal ions that form hydroxides with very low solubility product constants can easily combine with the hydroxyl groups on the surface of CDs. Thus, because of their high hydroxyl content, H-GQDs provide a large contact area with metal ions, and the addition of Cu^{2+}, Al^{3+}, Fe^{3+}, and Cr^{3+} to the H-GQD solution resulted in agglomeration, as shown in the TEM images (Fig. 7). Previous studies reported that the fluorescence properties of GQDs result from the quantum size and surface state effects [17]. For H-GQDs, the formation of large quantum dots due to agglomeration reduced the quantum size effect. The speeds of the agglomeration of H-GQDs in contact with Cu^{2+}, Al^{3+}, Fe^{3+}, and Cr^{3+} ions were different due to the difference in electrostatic force. Consequently, the sensitivities of H-GQDs for Cu^{2+}, Al^{3+}, Fe^{3+}, and Cr^{3+} ions were different. In addition, Liu *et al.* [39] reported that the strong electron-donating ability of hydroxyl groups is beneficial to fluorescence emission. Thus, the fluorescence quenching ability of H-GQDs was also derived from the destruction of the surface state due to the consumption of the surface hydroxyl groups. Our findings indicate that the surface hydroxyl groups of H-GQDs played a significant role in the detection of metal ions, providing a low detection limit, which makes these sensors suitable for application in the field of measurement.

4. Conclusions

(1) We prepared H-GQDs by introducing surface hydroxyl groups without changing the internal structure and other surface oxygen groups. The high hydroxyl content provided H-GQDs with excellent metal ions (namely, Cu^{2+}, Al^{3+}, Fe^{3+}, and Cr^{3+}) detection ability by fluorescence quenching, which is attributed to the aggregation and destruction of the surface state.

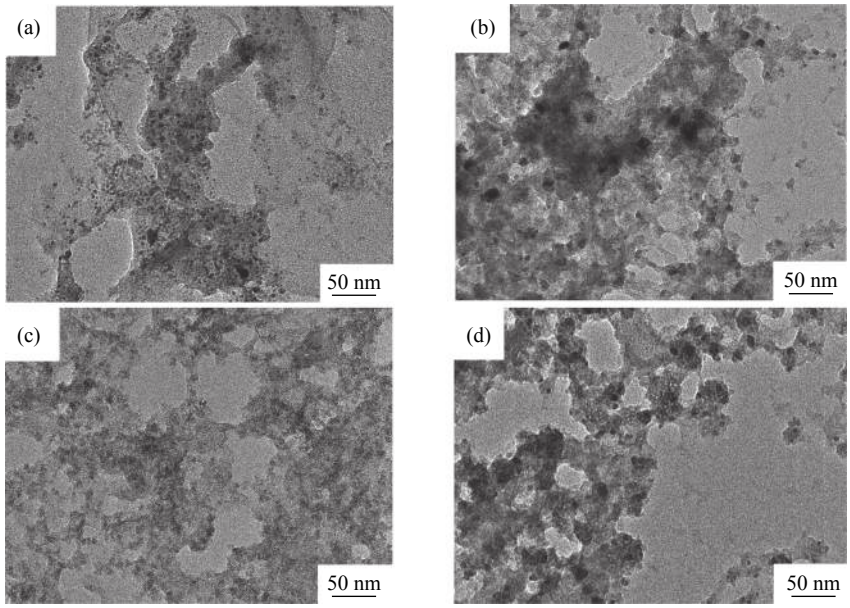

Fig. 7. TEM images of H-GQDs after addition of (a) Cu^{2+}, (b) Al^{3+}, (c) Fe^{3+}, and (d) Cr^{3+} ions.

(2) Compared with other non-reactive indicators based on carbon nanomaterials, H-GQDs provided a higher detection sensitivity, which meets the discharge standards for electroplating wastewater by WHO, suggesting their potential application for the determination of Cu^{2+}, Al^{3+}, Fe^{3+}, and Cr^{3+} in industrial wastewater.

Acknowledgements

This work was financially supported by the National Natural Science Foundation of China (No. 21674011) and Beijing Municipal Natural Science Foundation (No. 2172040).

References

[1] B. Li, Z.S. He, H.X. Zhou, H. Zhang, W. Li, T.Y. Cheng, and G.H. Liu, Reaction based colorimetric and fluorescence probes for selective detection of hydrazine, *Dyes Pigm.*, 146(2017), p. 300.

[2] J. Yao, M. Yang, and Y.X. Duan, Chemistry, biology, and medicine of fluorescent nanomaterials and related systems: newinsights into biosensing, bioimaging, genomics, diagnostics, and therapy, *Chem. Rev.*, 114(2014), No. 12, p. 6130.

[3] A.T. Aron, A.G. Reeves, and C.J. Chang, Activity-based sensing fluorescent probes for iron in biological systems, *Curr. Opin. Chem. Biol.*, 43(2018), p. 113.

[4] D.J. Cho and J.L. Sessler, Modern reaction-based indicator systems, *Chem. Soc. Rev.*, 38(2009), No. 6, p. 1647.

[5] P. Roy, P.C. Chen, A.P. Periasamy, Y.N. Chen, and H.T. Chang, Photoluminescent carbon nanodots: Synthesis, physicochemical properties and analytical applications, *Mater. Today*, 18(2014), No. 8, p. 447.

[6] J. Wen, Y.Q. Xu, H.J. Li, A.P. Lu, and S.G. Sun, Recent applications of carbon nanomaterials in fluorescence biosensing and bioimaging, *Chem. Commun.*, 51(2015), No. 57, p. 11346.

[7] Y.B. Song, S.J. Zhu, and B. Yang, Bioimaging based on fluorescent carbon dots, *RSC Adv.*, 4(2014), No. 52, p. 27184.

[8] L.P. Lin, X.H. Song, Y.Y. Chen, M.C. Rong, Y.R. Wang, L. Zhao, T.T. Zhao, and X. Chen, Europium-decorated graphene quantum dots as a fluorescent probe for label-free, rapid and sensitive detection of Cu^{2+} and l-cysteine, *Anal. Chim. Acta*, 891(2015), p. 261.

[9] Y. Li, X.Q. Liu, Q.Y. Li, J. Ge, H. Liu, S. Li, L.F. Wang, J. Wang, and N. Ma, Post-oxidation treated graphene quantum dots as a fluorescent probe for sensitive detection of copper ions, *Chem. Phys. Lett.*, 664(2016), p. 127.

[10] X.C. Fu, J.Z. Jin, J. Wu, J.C. Jin, and C.G. Xie, A novel "turn-on" fluorescence sensor for high selectively detecting Al (III) in aqueous solution based on simple electrochemical synthesized carbon dots, *Anal. Methods*, 9(2017), No. 26, p. 3941.

[11] K.G. Qu, J.S. Wang, J.S. Ren, and X.G. Qu, Carbon dots prepared by hydrothermal treatment of dopamine as an effective fluorescent sensing platform for the label-free detection of iron(III) ions and dopamine, *Chem. Eur. J.*, 19(2013), No. 22, p. 7243.

[12] B.J. Wang, S.J. Zhuo, L.Y. Chen, and Y.J. Zhang, Fluorescent graphene quantum dot nanoprobes for the sensitive and selective detection of mercury ions, *Spectrochim. Acta Part A*, 131(2014), p. 384.

[13] S. Sharma, A. Umar, S.K. Mehta, and S.K. Kansal, Fluorescent spongy carbon nanoglobules derived from pineapple juice: A potential sensing probe for specific and selective detection of chromium (VI) ions, *Ceram. Int.*, 43(2017), No. 9, p. 7011.

[14] F.X. Wang, Z.Y. Gu, W. Lei, W.J. Wang, X.F. Xia, and Q.L. Hao, Graphene quantum dots as a fluorescent sensing platform for highly efficient detection of copper(II) ions, *Sens. Actuators B*, 190(2014), p. 516.

[15] X.F. Niu, Y.B. Zhong, R. Chen, F. Wang, Y.J. Liu, and D. Luo, A "turn-on" fluorescence sensor for Pb^{2+} detection based on graphene quantum dots and gold nanoparticles, *Sens. Actuators B*, 255(2018), p. 1577.

[16] S.H. Zhou, H.B. Xu, W. Gan, and Q.H. Yuan, Graphene quantum dots: Recent progress in preparation and fluorescence sensing applications, *RSC Adv.*, 6(2016), No. 112, p. 110775.

[17] S.J. Zhu, J.H. Zhang, C.Y. Qiao, S.J. Tang, Y.F. Li, W.J. Yuan, B. Li, L. Tian, F. Liu, R. Hu, H.N. Gao, H.T. Wei, H. Zhang, H.C. Sun, and B. Yang, Strongly green-photoluminescent graphene quantum dots for bioimaging applications, *Chem. Commun.*, 47(2011), No. 24, p. 6858.

[18] Y.Q. Feng, J.P. Zhao, X.B. Yan, F.L. Tang, and Q.J. Xue, Enhancement in the fluorescence of graphene quantum dots by hydrazine hydrate reduction, *Carbon*, 66(2014), No. 1, p. 334.

[19] Z.S. Qian, X.Y. Shan, L.J. Chai, J.R. Chen, and H. Feng, A fluorescent nanosensor based on graphene quantum dots–aptamer probe and graphene oxide platform for detection of lead (II) ion, *Biosens. Bioelectron.*, 68(2015), p. 225.

[20] Y. Li, X.Q. Liu, J. Wang, H. Liu, S. Li, Y.B. Hou, W. Wan, W.D. Xue, N. Ma, and J.Z. Zhang, Chemical nature of redox-controlled photoluminescence of graphene quantum dots by post-synthesis treatment, *J. Phys. Chem. C*, 120(2016), No. 45, p. 26004.

[21] Y. Li, H. Liu, X.Q. Liu, S. Li, L.F. Wang, N. Ma, and D.L. Qiu, Free-radical-assisted rapid synthesis of graphene quantum dots and their oxidizability studies, *Langmuir*, 32(2016), No. 34, p. 8641.

[22] P.H. Luo, Y. Qiu, X.F. Guan, and L.Q. Jiang, Regulation of photoluminescence properties of graphene quantum dots via hydrothermal treatment, *Phys. Chem. Chem. Phys.*, 16(2014), No. 35, p. 19011.

[23] S.J. Zhu, J.H. Zhang, S.J. Tang, C.Y. Qiao, L. Wang, H.Y. Wang, X. Liu, B. Li, Y.F. Li, W.L. Yu, X.F. Wang, H.C. Sun, and B. Yang, Surface chemistry routes to modulate the

photoluminescence of graphene quantum dots: From fluorescence mechanism to up-conversion bioimaging applications, *Adv. Funct. Mater.*, 22(2012), No. 22, p. 4732.

[24] L.L. Li, G.H. Wu, G.H. Yang, J. Peng, J.W. Zhao, and J.J. Zhu, Focusing on luminescent graphene quantum dots: Current status and future perspectives, *Nanoscale*, 10(2013), No. 5, p. 4015.

[25] S.L. Hu, A. Trinchi, P. Atkin, and I. Cole, Tunable photoluminescence across the entire visible spectrum from carbon dots excited by white light, *Angew. Chem. Int. Ed.*, 54(2015), No. 10, p. 2970.

[26] T.J. Fan, W.J. Zeng, W. Tang, C.Q. Yuan, S.Z. Tong, K.Y. Cai, Y.D. Liu, W. Huang, Y. Min, and A.J. Epstein, Controllable size-selective method to prepare graphene quantum dots from graphene oxide, *Nanoscale Res. Lett.*, 10(2015), No. 19, p. 55.

[27] J.R. Lakowicz, *Principles of Fluorescence Spectroscopy*, 3rd Ed., Springer Science+Business Media, LLC, New York, 2006.

[28] C.Q. Zhang, Y. Yan, Q.H. Pan, L.B. Sun, H.M. He, Y.L. Liu, Z.Q. Liang, and J.Y. Li, A microporous lanthanum metal-organic framework as a bi-functional chemosensor for the detection of picric acid and Fe^{3+} ions, *Dalton Trans.*, 44(2015), No. 29, p. 13340.

[29] X.H. Zhou, L. Li, H.H. Li, A. Li, T. Yang, and W. Huang, A flexible Eu(III)-based metal-organic framework: Turn-off luminescent sensor for the detection of Fe(III) and picric acid, *Dalton Trans.*, 42(2013), No. 34, p. 12403.

[30] X.Q. Dong, C.L. Li, J. Li, W.T. Huang, J. Wang, and R.B. Liao, Application of a system dynamics approach for assessment of the impact of regulations on cleaner production in the electroplating industry in China, *J. Cleaner Prod.*, 20(2012), No. 1, p. 72.

[31] L. Shi, J.S. Shi, and Y. Shi, Discussion on the emission standard of pollutants for electroplating, *Electroplat. Finish.*, 28(2009), No. 5, p. 44.

[32] C. Shen, S.Y. Ge, Y.Y. Pang, F.N. Xi, J.Y. Liu, X.P. Dong, and P. Chen, Facile and scalable preparation of highly luminescent N,S co-doped graphene quantum dots and their application for parallel detection of multiple metal ions, *J. Mater. Chem. B*, 5(2017), No. 32, p. 6593.

[33] X.F. Liu, W. Gao, X.M. Zhou, and Y.Y. Ma, Pristine graphene quantum dots for detection of copper ions, *J. Mater. Res.*, 29(2014), No. 13, p. 1401.

[34] V. Dujols, F. Ford, and A.W. Czarnik, A long-wavelength fluorescent chemodosimeter selective for Cu(II) ion in water, *J. Am. Chem. Soc.*, 119(1997), No. 31, p. 7386.

[35] L. Fan, J.C. Qin, T.R. Li, B.D. Wang, and Z.Y. Yang, A novel rhodamine chromone-based "Off-On" chemo sensor for the differential detection of Al(III) and Zn(II) in aqueous solutions, *Sens. Actuators B*, 203(2014), No. 14, p. 550.

[36] D. Wang, L. Wang, X.Y. Dong, Z. Shi, and J. Jin, Chemically tailoring graphene oxides into fluorescent nanosheets for Fe^{3+} ion detection, *Carbon*, 50(2012), No. 6, p. 2147.

[37] J. Ju and W. Chen, Synthesis of highly fluorescent nitrogen-doped graphene quantum dots for sensitive, label-free detection of Fe (III) in aqueous media, *Biosens. Bioelectron.*, 58(2014), p. 219.

[38] C. Yi, W.W. Tian, B. Song, Y.P. Zheng, Z.J. Qi, Q. Qi, and Y.M. Sun, A new turn-off fluorescent chemosensor for iron (III) based on new diphenylfluorenes with phosphonic acid, *J. Lumin.*, 141(2013), p. 15.

[39] L.Q Liu, Y.F Li, L. Zhan, Y. Liu, and C.Z. Huang, One-step synthesis of fluorescent hydroxyls-coated carbon dots with hydrothermal reaction and its application to optical sensing of metal ions, *Sci. China Chem.*, 54(2011), No. 8, p. 1342.

[40] Y.F. Chen, C.L. Kao, P.C. Huang, C.Y. Hsu, and C.H. Kuei, Facile synthesis of multi-responsive functional graphene quantum dots for sensing metal cations, *RSC Adv.*, 6(2016), No. 105, p. 103006.

[41] J.W. Xin, L.J. Miao, S.G. Chen, and A.G. Wu, Colorimetric detection of Cr^{3+} using tripolyphosphate modified gold nanoparticles in aqueous solutions, *Anal. Methods*, 4(2012), No. 5, p. 1259.

[42] H. Huang, Y.H. Weng, L.H. Zheng, B.X. Yao, W. Weng, and X.C. Lin, Nitrogen-doped carbon quantum dots as fluorescent probe for “off-on” detection of mercury ions, L-cysteine and iodide ions, *J. Colloid Interface Sci.*, 506(2017), p. 373.